# Self-association and hydrogen bonding of propionaldehyde in binary mixtures with water and methanol investigated by concentration-dependent polarized Raman study and DFT calculatio...

**ARTICLE** *in* JOURNAL OF RAMAN SPECTROSCOPY · APRIL 2011

Impact Factor: 2.67 · DOI: 10.1002/jrs.2779

Research Article

Journal of RAMAN SPECTROSCOPY

Received: 16 March 2010 Accepted: 15 July 2010 Published online in Wiley Online Library: 28 August 2010

(wileyonlinelibrary.com) DOI 10.1002/jrs.2779

# Self-association and hydrogen bonding of propionaldehyde in binary mixtures with water and methanol investigated by concentration-dependent polarized Raman study and DFT calculations

**Dheeraj K. Singh,[a] Sunil K. Srivastava,[b] S. Schlücker,[b] Ranjan K. Singh[a] and B. P. Asthana[a]***

**The Raman spectra of neat propionaldehyde [$CH_3CH_2CHO$ or propanal (Pr)] and its binary mixtures with hydrogen-donor solvents, water (W) and methanol (M), [$CH_3CH_2CHO + H_2O$] and $CH_3CH_2CHO + CH_3OH$] with different mole fractions of the reference system, Pr varying from 0.1 to 0.9 at a regular interval of 0.1, were recorded in the $\nu$(C═O) stretching region, 1600–1800 $cm^{-1}$. The isotropic parts of the Raman spectra were analyzed for both the cases. The wavenumber positions and line widths of the component bands were determined by a rigorous line-shape analysis, and the peaks corresponding to self-associated and hydrogen-bonded species were identified. Raman peak at ~1721 $cm^{-1}$ in neat Pr, which has been attributed to the self-associated species, downshifts slightly (~1 $cm^{-1}$) in going from mole fraction 0.9 to 0.6 in (Pr + W) binary mixture, but on further dilution it shows a sudden downshift of ~7 $cm^{-1}$. This has been attributed to the low solubility of Pr in W (~30%), which does not permit a hydrogen-bonded network to form at higher concentrations of Pr. A significant decrease in the intensity of this peak in the Raman spectra of Pr in a nonpolar solvent, *n*-heptane, at high dilution ($C = 0.05$) further confirms that this peak corresponds to the self-associated species. In case of the (Pr + M) binary mixture, however, the spectral changes with concentration show a rather regular trend and no special features were observed.** 

**Keywords:** hydrogen bonding; self-association; binary mixture [($CH_3CH_2CHO + H_2O/CH_3OH$)]; polarized Raman study; DFT calculations

## Introduction

Hydrogen bonding, which is of fundamental significance for chemical structures and reactivity,[1] is an extensively investigated aspect,[2,3] especially due to its importance for biological systems. It is the key to understand the structure and properties of water (W), proteins and DNA, which are the building blocks of life. A major aspect of current interest is its role in molecular recognition by nucleic acids, proteins and small molecules.[4] Various experimental methods are employed to characterize hydrogen bonds. For the solid state, NMR spectroscopy is one of the preferred methods.[5] In the gas phase, vibrational spectroscopy on molecular beams is often used, which allows one to assess information on isolated hydrogen-bonded complexes.[6] In the liquid state, where the formation and cleavage of such complexes occurs rapidly, vibrational spectroscopy is most suited to study hydrogen bonding[2] since this can reveal both structural and dynamic aspects[2,7] in the liquid phase. The line width contains information about molecular dynamics, whereas the wavenumber position of a vibrational band is related to the corresponding force constant, which depends basically on electronic structure and bonding.

The carbonyl group (C═O) present in aldehydes, ketones, carboxylic acids, esters, amides and a few other class of compounds plays a major role in many biological processes and often is of great interest for industrial purposes also. Experimental studies on aldehyde-based compounds were discussed quite early in a review,[8] and also a few theoretical studies were dedicated earlier to this subject.[9–11] Propanal (Pr) is a saturated 3-carbon aldehyde and is a structural isomer of acetone. The liquid spectra of Pr and butylaldehyde with varying temperature were studied earlier by Sbrana and Schettino.[12] In that study, the enthalpy difference between the possible isomers was measured and the vibrational assignments of the conformer stable in the crystalline form were reported. Later, the IR spectrum of Pr was also recorded by Van Nuffel *et al*.[13] These authors proposed assignments for the *cis* and *gauche* conformers.

A few quantum chemical calculations were also performed[13–16] on different conformers of Pr for varying values of the dihedral angle defining the torsion of the aldehydic group. Almost a decade ago, Kolandaivel *et al*.[17] reported the molecular

* *Correspondence to: B. P. Asthana, Laser and Spectroscopy Laboratory, Department of Physics, Banaras Hindu University, Varanasi-221005, India. E-mail: bpasthana@rediffmail.com; bpasthana@gmail.com*

a *Laser and Spectroscopy Laboratory, Department of Physics, Banaras Hindu University, Varanasi 221005, India*

b *Fachbereich Physik, Universität Osnabrück, D-49076 Osnabrück, Germany*

 

structure and conformational stability of the *E* and *Z* geometrical isomers of propionaldehyde oxime by using the *ab initio* and density functional theory (DFT) methods. The SPASIBA vibrational spectroscopic force field (developed for aldehyde) was used by Zanoun *et al.*[18] to study the structure and vibrational wavenumber of methanol (M), ethanol and Pr, and they were able to reproduce the conformational energies, observed structures and wavenumbers of the normal vibrational modes. Kudich *et al.*[19] studied the potential energy surface of the conformationally non-rigid Pr molecule in the lowest excited triplet ($T_1$) and singlet ($S_1$) electronic states calculated by the multiconfigurational self-consistent field method CASSCF. Recently, Hwa Kim *et al.*[20], through *ab initio* calculations at the B3LYP/6-311++G** level, found that the *gauche* conformer was slightly more stable, with the energy difference between the two conformers determined to be only 65 $cm^{-1}$. In another recent study, Villa *et al.*[21] performed the zero-point vibrational energy (ZPVE) correction to the energy and calculated the asymmetric aldehydic and methyl torsion spectra for the deuterated Pr, for which observed spectra had already been studied. In the case of the aldehydic torsion, the ZPEV correction was essential and the fundamental frequencies thus obtained for the studied species were able to reproduce the experimental data precisely. Most recently, Choi *et al.*[22] reported two different conformational isomers of Pr, *cis* and *gauche*, which were investigated by the vacuum-UV mass-analyzed threshold ionization (VUV-MATI) spectroscopy.

Thus, a survey of the literature reveals that several studies on Pr have been made using different experimental and theoretical techniques.[13–21] However, detailed studies of the hydrogen-bonding properties and various hydrogen-bonded complexes of Pr in polar/nonpolar solvents are lacking so far. In view of the above-mentioned studies and foregoing discussions, it was thought worthwhile to study the different binary complexes of Pr with M and W. Pr was chosen for the present study as a model system of a basic aldehydic compound, and the spectra of neat Pr as well as binary mixtures in two most important solvents present in biological systems were studied. In the present study, we have taken the $\nu$(C═O) stretching vibration (~1700–1750 $cm^{-1}$ in this case) of Pr as the marker band and the changes in the spectral features are studied as a function of concentration of the reference system, Pr. DFT calculations on optimized geometry and vibrational wavenumbers of the complexes with different stoichiometric ratios of Pr and the solvent were performed. The results thus obtained were used to interpret the observed spectral features and their variation with concentration.

## Experimental

Pr and M were purchased from Fluka and used without any further purification. Deionized, distilled W was used for preparing the mixtures. A Spex-1404 double monochromator with 2400 grooves/mm gratings and equipped with a liquid-$N_2$-cooled CCD detector (Photometric model SDS 9000) was used to record the spectra. The 514.5 nm line of an $Ar^+$-ion laser with an output power of 1 W (watt) was used as the excitation source. Polarized Raman measurement was performed in order to get pure vibrational information by calculating the isotropic part of the Raman spectra. The setup used for polarized Raman measurements was carefully checked by measuring the depolarization ratios of the 459, 315 and 218 $cm^{-1}$ bands of $CCl_4$. The values of the depolarization ratios for these three Raman bands were measured to be <0.01, 0.75 and 0.75, respectively. This was essential to ensure that the instrument was properly set for making polarization measurements. The data acquisition time for each spectrum was 25–50 s per window. The spectral resolution was better than 0.5 $cm^{-1}$ in the present setup. The parallel ($I_{||}$) and perpendicular ($I_{\perp}$) components of the Raman spectra were recorded in the $\nu$(C═O) stretching region, 1600–1800 $cm^{-1}$, at different mole fractions ($C$ = 0.1–0.9 at a regular interval of 0.1) of Pr in the binary mixtures (Pr + W) and (Pr + M). However, Pr has low solubility (20–30%) in W but good solubility in M.

Isotropic and anisotropic parts of the Raman spectra were calculated using the following relationships:

$$I_{iso}(\omega) = I_{||}(\omega) - 4/3\, I_{\perp}(\omega) \quad (1)$$

$$I_{anis}(\omega) = I_{\perp}(\omega) \quad (2)$$

where $I_{||}$ and $I_{\perp}$ are the experimentally measured parallel and perpendicular components of the Raman scattered intensities, respectively. $I_{iso}(\omega)$ is the isotropic contribution, which is directly related to the vibrational dephasing, and $I_{anis}(\omega)$ is the anisotropic contribution to the Raman line profile due to reorientational motion. In recent years, this idea has extensively been applied to study vibrational dephasing in many associated/non-associated systems and this aspect of Raman spectroscopic technique has frequently been employed, particularly to study self-associated and hydrogen-bonded systems.[23–28]

## Computational Details

All the theoretical calculations were performed using Gaussian 03 program package.[29] The optimized gas-phase geometrical structures and vibrational wavenumbers of the Pr monomer, dimer(s) and its various hydrogen-bonded complexes with W and M were calculated using DFT with the hybrid functional that mixes the Lee, Yang and Parr functional for the exchange correlation (B3LYP).[30,31] In two of our recent studies[32,33] also, we performed DFT calculations using B3LYP functional and this was quite helpful to draw some meaningful conclusions from the experimental results. Apart from the gas-phase calculation, we also calculated the solvated structures in order to realize a condition quite close to that of the experiment. In doing so, the optimized gas-phase structures were used as the input structures and the polarizable continuum model (PCM)[34] solvation method was used for the calculations without applying any constraints. All the optimized structures were finally at the minimum of the potential surface, which was inferred from the absence of negative (imaginary) wavenumbers. All the possible structures and the corresponding parameters, such as C═O bond lengths, $\nu$(C═O) stretching wavenumbers and hydrogen-bond distances for the different complexes, are reported in Table 1.

## Results and Discussions

### Raman spectra of Pr in W and M

The isotropic part of the Raman spectra of neat Pr and nine other binary mixtures of (Pr + W) and (Pr + M) with mole fractions $C$ = 0.9, 0.8, 0.7, 0.6, 0.5, 0.4, 0.3, 0.2 and 0.1 of Pr, in the region 1600–1800 $cm^{-1}$, are presented in Figs 1 and 2, respectively. In the Raman spectra of neat Pr, there are three bands in the $\nu$(C═O)

Journal of RAMAN SPECTROSCOPY

**Table 1.** Optimized bond distances and calculated wavenumbers for $\nu$(C═O) vibration in neat Pr, different complexes of propanal (Pr) with water (W)/methanol (M) in gas phase as well as solvated structures (both bulk and specific + bulk solvation)

| | Bond lengths (Å) | | | | | |
|---|---|---|---|---|---|---|
| Molecular systems | $O\cdots H_a$ ($O\cdots H_b$) [$O_a\cdots H_c$] | $O_a\cdots H$ ($O_b\cdots H_d$) [$O_c\cdots H$] | $O_a\cdots H'$ ($O'\cdots H_b$) [$O_b\cdots H$] | $O\cdots H'$ ($O'\cdots H$) [$O_c\cdots H_d$] | C═O (C′═O′) | Wavenumber ($cm^{-1}$) $\nu$(C═O) |
| Pr | – | – | – | – | 1.206 | 1803 |
| Pr(self1) | – | – | – | 2.56 | 1.211 | 1774 |
| | | | | (2.56) | (1.211) | |
| Pr(self2) | – | – | – | 2.51 | 1.209 | 1788 |
| | | | | (2.51) | (1.209) | |
| Pr $W_1$ | 1.94 | 3.02 | – | – | 1.212 | 1783 |
| Pr $W_2$ | 1.94 | 2.84 | – | – | 1.218 | 1761 |
| | (1.94) | (2.52) | | | | |
| Pr $W_3$ | 1.88 | – | – | – | 1.223 | 1738 |
| | (1.95) | (2.57) | | | | |
| | [1.86] | [2.29] | | | | |
| $Pr_2$ $W_2$ | 1.86 | – | 2.25 | | 1.218 | 1760 |
| | | | (1.86) | | (1.218) | |
| | | | [2.25] | | | |
| Pr–W(Sol)[a] | – | – | – | – | 1.216 | 1753 |
| Pr–$W_1$(Sol)[b] | 1.90 | 3.60 | – | – | 1.219 | 1741 |
| Pr–$W_2$(Sol)[b] | 1.92 | | 3.60 | – | 1.222 | 1731 |
| | (1.94) | (3.28) | | | | |
| Pr $M_1$ | 1.95 | 3.08 | – | – | 1.212 | 1783 |
| Pr $M_2$ | 1.98 | 2.84 | – | – | 1.218 | 1760 |
| | (1.98) | 2.52 | | | | |
| Pr $M_3$ | 1.98 | 2.86 | – | – | 1.220 | 1753 |
| | (1.90) | | | [2.34] | | |
| $Pr_2$ $M_2$ | 1.87 | – | 2.25 | – | 1.218 | 1759 |
| | 1.87 | | | (1.22) | | |
| | | | 2.25 | | | |
| Pr M(Sol)[a] | – | – | – | – | 1.215 | 1753 |
| Pr $M_1$(Sol)[b] | 1.88 | 3.61 | – | – | 1.219 | 1741 |

[a] Bulk solvation.
[b] (specific + bulk) solvation.

stretching region as shown in Fig. 1. There is one weak band at ~1690 $cm^{-1}$ and one intense doublet at ~1725 $cm^{-1}$. The two components of the doublet at 1721.6 and 1731.8 $cm^{-1}$ for neat Pr (Table 2), which are basically $\nu$(C═O) vibrations, essentially correspond to two species, namely self-associated Pr and the isolated Pr, respectively. In order to confirm that the peak at ~1721 $cm^{-1}$ corresponded to the C═O stretching in the self-associated Pr, we performed a Raman measurement on the binary mixture of Pr with the noninteracting solvent *n*-heptane, taking different mole fractions of Pr. It is to be noted that *n*-heptane, which has molecular formula $H_3C$-$(CH_2)_5$-$CH_3$ with a linear chain of seven carbon atoms, is quite neutral and it has no hydrogen-bonding capability with Pr. It was observed that the intensity of the Raman band at ~1721 $cm^{-1}$ slowly goes on decreasing with dilution by *n*-heptane. The spectra for some selected mole fraction of Pr, i.e. $C = 1.00$ (neat), 0.5, 0.1 and 0.05, are presented in Fig. 3. It is evident that at an extreme dilution ($C = 0.05$), the intensity of the band at ~1721 $cm^{-1}$ is significantly reduced and a sharp peak at ~1732 $cm^{-1}$ is observed, which can therefore be easily assigned to the C═O stretching vibration of isolated Pr. This drastic decrease in the intensity of the ~1721 $cm^{-1}$ band essentially indicates that due to the excess of *n*-heptane, the self-associated networks of Pr molecules are disrupted and consequently the intensity of the band corresponding to the self-associated species (~1721 $cm^{-1}$) diminishes. This also confirms our assignment of the band at ~1721 $cm^{-1}$ to the self-associated species.

On dilution with W up to 0.6 mole fraction, a slight spectral change is observed, which is quite expected since in this range the Pr solubility is poor (20–30%) and therefore a large number of Pr molecules and a relatively small number of W molecules are available. A sudden spectral change is observed at mole fraction 0.5, where the doublet is shifted toward the lower wavenumber side and a new band at ~1713 $cm^{-1}$ also appears on the lower wavenumber side. The intensity of this newly developed band goes on increasing on dilution (Fig. 1), indicating that this band corresponds to the hydrogen-bonded species.

In case of the (Pr + M) mixture, a consistent variation in spectral feature is observed upon dilution with M since Pr is fully soluble in M and the extent of solubility is not an issue. The doublet feature slowly disappears in this case and a new band is observed at a lower wavenumber (~1719 $cm^{-1}$, Fig. 2). The intensity of this new band also goes on increasing with dilution and this clearly shows that the hydrogen-bonded species with M is predominant



  

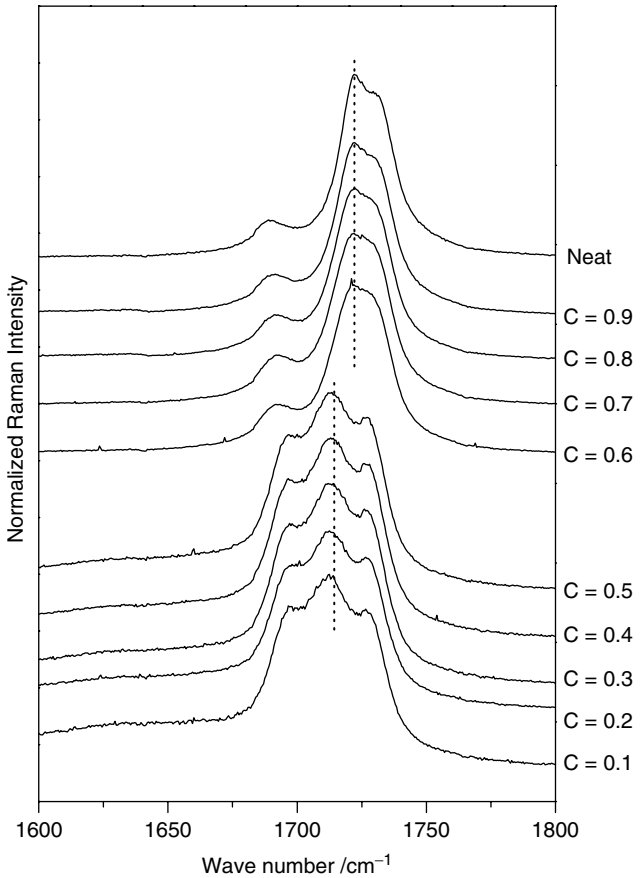


**Figure 1.** Isotropic part of the Raman spectra of propanal (Pr) measured in the C═O stretching region in neat Pr and nine different mole fractions $C$ = 0.1, 0.2, 0.3, 0.4, 0.5, 0.6, 0.7, 0.8 and 0.9 of the reference system Pr in the [Pr + W] binary mixture.

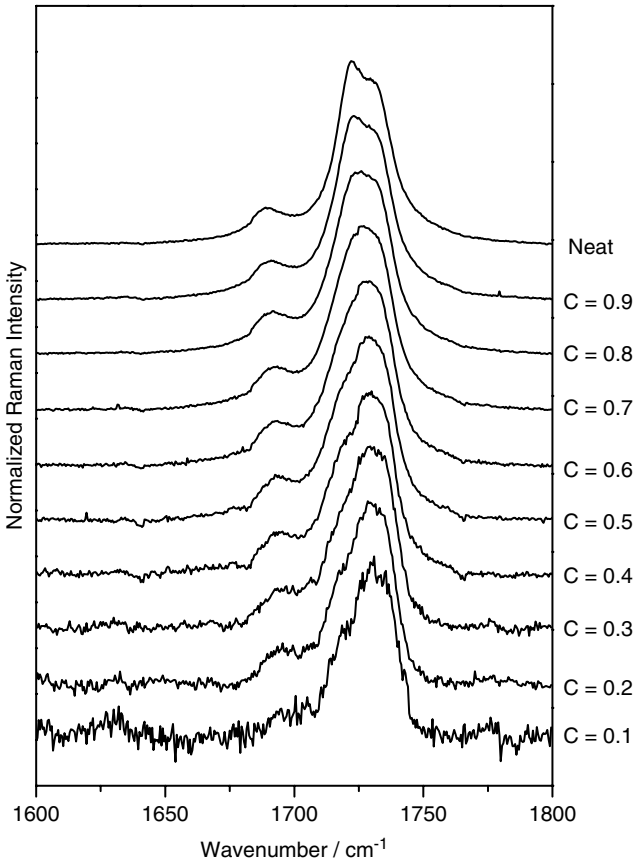


**Figure 2.** Isotropic part of the Raman spectra of propanal (Pr) measured in the C═O stretching region in neat Pr and nine different mole fractions $C$ = 0.1, 0.2, 0.3, 0.4, 0.5, 0.6, 0.7, 0.8 and 0.9 of the reference system Pr in the [Pr + M] binary mixture.

in comparison to self-associated species in the case of the (Pr + M) binary mixture.

## Optimized structures and correlation with the experimental results

*Propanal–water*

DFT calculations were performed in the gas phase in order to calculate the optimized energy and vibrational wavenumbers of the isolated Pr and self-associated species in two configurations, namely end-on and antiparallel, as shown in Fig. 4(b) and (c), respectively. The calculations were also performed for two different hydrogen bonded Pr–W species, namely $Pr_2W_2$ and $PrW_3$, as shown in Fig. 4(d) and (e), respectively. The optimized hydrogen-bond distances and the calculated wavenumbers for the different structures are given in Table 1 and also shown in Fig. 4. The self-associated structure in the antiparallel configuration shown in Fig. 4(c) has a relatively strong hydrogen bond (2.51 Å) compared to the end-on configuration (2.56 Å). However, there is a very small energy difference of 0.06 kcal/mol between the antiparallel and end-on configurations, the antiparallel configuration having a lower energy. Thus it is quite likely that both the self-associated structures may be present in some kind of equilibrium. When W molecules are added to the reference system Pr, a sudden change is observed in the Raman spectra, which can be explained in terms of interaction of the W molecule with the self-associated Pr network. It is very likely that W interacts with the end-on self-associated network owing to weaker hydrogen bonds. Hence, on dilution, around $C$ = 0.5 mole fraction of Pr, where Pr and W have equal proportion, a $Pr_2W_2$ network shown in Fig. 4(d) may cause a significant change in the Raman spectra. The doublet peak of $\nu$(C═O) stretching vibration is altogether red-shifted and a new peak is observed due to the hydrogen-bonding network. The intensity of this new peak due to hydrogen-bonded network goes on increasing with increasing dilution with W and this is a clear indication that this band was due to the hydrogen-bonded species.

*Propanal–methanol*

Optimized structures and vibrational wavenumbers of Pr and its hydrogen-bonded structures with M were calculated in order to explain the observed spectral changes. The hydrogen-bonded complexes with two Pr and two M molecules ($Pr_2M_2$) as well as one Pr molecule with three M molecules ($PrM_3$) were optimized, and the structures obtained are shown in Fig. 4(f) and (g), respectively. In principle, there is a possibility of forming the hydrogen-bonding network $Pr_2M_2$ similar to that with the W molecule ($Pr_2W_2$), and the presence of methyl group in M, which usually causes steric hindrance to the neighboring molecule, is not so effective since the $CH_3$ group lies on the periphery of the network as shown in Fig. 4(f). Hence, the hydrogen-bonding network $Pr_2M_2$ is almost equally probable, whereas in case of W, there is no such steric hindrance

Journal of RAMAN SPECTROSCOPY

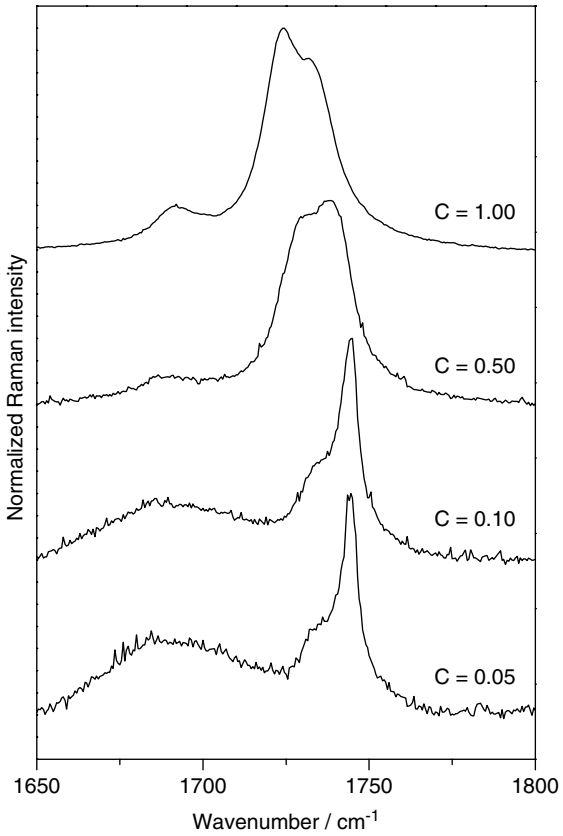


**Figure 3.** Raman spectra of Pr measured in the C═O stretching region at four different mole fractions $C$ = 1.0, 0.5, 0.1 and 0.05 of Pr in the [Pr + *n*-heptane] binary mixture.

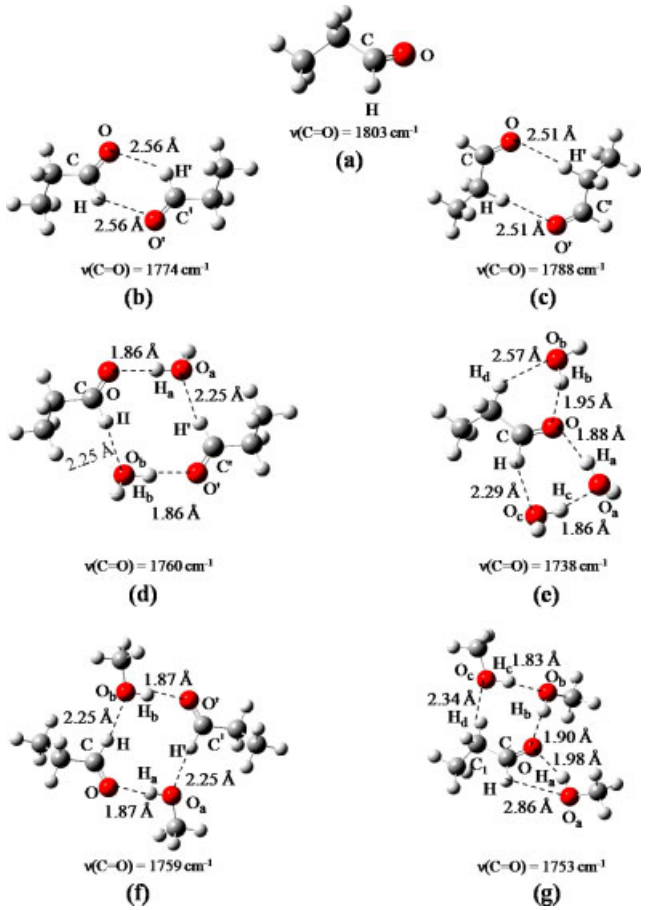


**Figure 4.** Optimized geometries of propanal (Pr), its self-associated structures and different hydrogen-bonded complexes with water (W) and methanol (M): (a) Pr; (b) $Pr_2$ (end-on configuration); (c) $Pr_2$ (antiparallel configuration); (d) $Pr_2$ $W_2$; (e) $PrW_3$; (f) $Pr_2M_2$ and (g) $PrM_3$.

and, also due to stronger hydrogen-bonding capability of W, the $Pr_2$ $W_2$ network is easily formed. The disappearance of the doublet nature of the $\nu$(C═O) stretching vibrational band in case of the (Pr + M) mixture can be easily explained in terms of decreasing self-associated network of Pr in presence of M molecules. As the self-associated network of Pr breaks, more and more M molecules may come in contact with Pr molecules and form a complex, such as $PrM_3$ shown in Fig. 4(g). Due to the formation of such a complex, an additional band may appear at lower wavenumber corresponding to this hydrogen-bonded complex.

### Line-shape analysis of the Raman spectra for the $\nu$(C═O) Raman band in (Pr + W) and (Pr + M) binary mixtures

The isotropic part of the Raman spectra of neat Pr and nine other binary mixtures of both (Pr + W) and (Pr + M) with mole fractions $C$ = 0.9, 0.8, 0.7, 0.6, 0.5, 0.4, 0.3, 0.2 and 0.1 of Pr in the region 1600–1800 $cm^{-1}$ was analyzed using the curve-fitting program Spectra Calc. The analyzed Raman spectra along with the component bands for the mole fractions 1.0, 0.9, 0.7, 0.5, 0.3 and 0.1 for binary mixtures (Pr + W) and 1.0, 0.9, 0.7, 0.5, 0.3 and 0.2 for binary mixtures (Pr + M) are presented in Figs 5 and 6, respectively. The change in the intensities of the component bands corresponding to self-associated and hydrogen-bonded complexes is also clearly seen in Figs 5 and 6. The peak positions and line widths for each analyzed component of the spectra of (Pr + W) and (Pr + M) mixtures are given in Tables 2 and 3, respectively. The variation of peak positions and line widths of the deconvoluted doublet peak for $\nu$(C═O) stretching mode of Pr with its varying mole fraction in binary mixtures with W are plotted as a function of concentration of Pr (in mole fraction) in Fig. 7. The changes in the spectral feature in the binary mixture (Pr + M) do not show any peculiar trend, probably due to the high solubility of Pr in M, and hence their variation is not presented pictorially.

The Raman peak at ~1721 $cm^{-1}$, which is due to the $\nu$(C═O) stretching vibration of the self-associated dimer, shows a slight downshift (~1 $cm^{-1}$) upon dilution with W up to 0.6 mole fraction of Pr. On further dilution, a sudden shift of ~7 $cm^{-1}$ is observed, whereas the band at ~1731 $cm^{-1}$, which corresponds to the isolated Pr molecule, shows a downshift of ~3 $cm^{-1}$ in the whole concentration range. This is what should be expected since at higher mole fractions ($C$ = 0.9–0.6) of Pr, only a small fraction of Pr molecules is soluble due to low solubility in W (20–30%). Consequently, relatively few Pr molecules may form hydrogen bond with the W molecule and the hydrogen-bonded species experiences a very small perturbation, which causes a small wavenumber shift of ~1 $cm^{-1}$. At a mole fraction $C$ = 0.5 and below, a larger proportion of Pr molecules is soluble in W, which obviously forms more number of hydrogen-bonded networks. In this situation, a hydrogen-bonding network as shown in Fig. 4(d) is more probable. As a consequence, the self-associated complex of Pr is now mediated through W molecules and consequently a larger perturbation is caused, such that the band due to self-association, which was observed in neat Pr at ~1721 $cm^{-1}$, shows a sudden



  

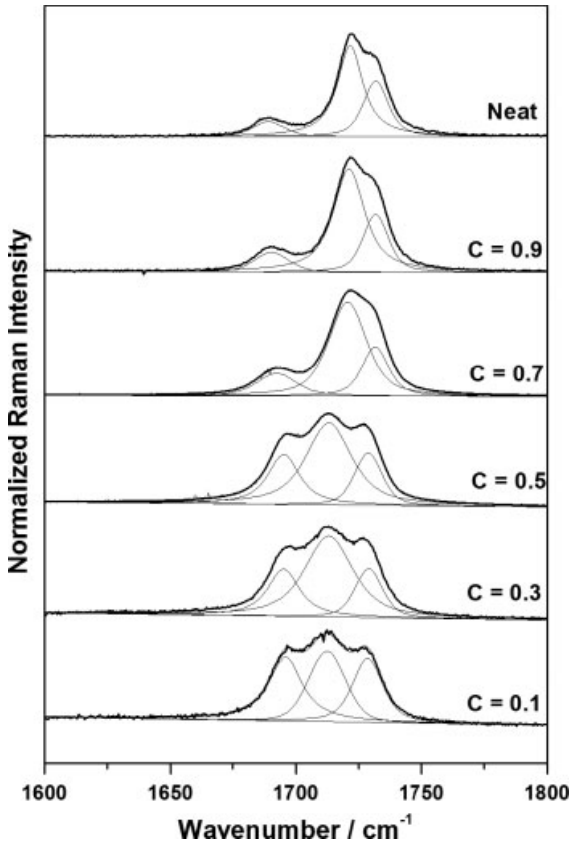


**Figure 5.** Analyzed component bands in the Raman spectra of neat Pr and its binary mixtures [Pr + W] in the C=O stretching region at five different mole fractions of Pr $C = 0.1, 0.3, 0.5, 0.7$ and 0.9.

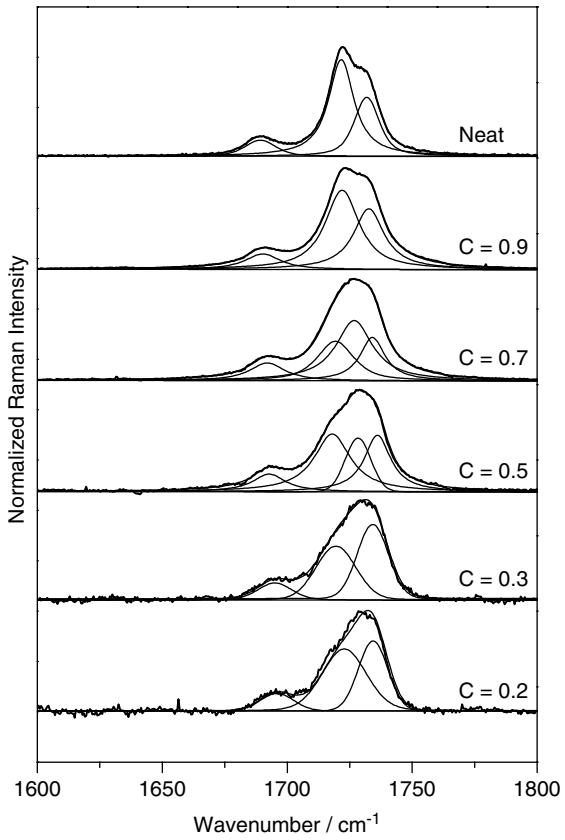


**Figure 6.** Analyzed component bands in the Raman spectra of neat Pr and its binary mixtures [Pr + M] in the C=O stretching region at five different mole fractions of Pr $C = 0.2, 0.3, 0.5, 0.7$ and 0.9.

downshift of $\sim$7 $cm^{-1}$. This sudden shift is also evident from the calculated vibrational wavenumber of the $\nu$(C=O) stretching vibration for the $Pr_2W_2$ complex, which appears at 1760 $cm^{-1}$ as compared to the $\nu$(C=O) stretching vibration for the self-associated $Pr_2$ molecule at 1774 $cm^{-1}$. If one looks at the trend of the concentration-dependent line width variation of this Raman band, it first shows a broadening ($\sim$10 $cm^{-1}$) up to mole fraction 0.5, and on further dilution it shows an apparent narrowing with line width going to $\sim$4 $cm^{-1}$. This essentially means that at higher mole fraction of Pr, where the number of hydrogen-bonded species is much less due to the small number of W molecules, the diffusion of Pr molecules causes the broadening. But at higher dilutions (mole fraction 0.5 and below), due to a large number of W molecules becoming available for making Pr–W complexation, a decrease in line width is observed owing to the tightening of the hydrogen-bonding network, which leads to motional narrowing.[35] On the other hand, the band at $\sim$1731 $cm^{-1}$, which is attributed to the $\nu$(C=O) stretching vibration of the isolated Pr molecule, shows a consistent broadening of $\sim$2.5 $cm^{-1}$ due to increasing diffusion effect.[36]

**Table 2.** Wavenumber positions and line widths of the three Raman peaks obtained by analyzing the observed isotropic Raman line profile in the $\nu$(C=O) region at different concentrations in mole fraction, C of propanal in the (Pr + W) binary mixture

| Mole fraction (*C*) (propanal) | Peak 1 | | Peak 2 $(C{=}O)_{HB}$ | | Peak 3 $(C{=}O)_{SA}$ | | Peak 4 $(C{=}O)_{ISO}$ | |
|---|---|---|---|---|---|---|---|---|
| | $\nu$ ($cm^{-1}$) | $\Gamma_{FWHM}$ ($cm^{-1}$) | $\nu$ ($cm^{-1}$) | $\Gamma_{FWHM}$ ($cm^{-1}$) | $\nu$ ($cm^{-1}$) | $\Gamma_{FWHM}$ ($cm^{-1}$) | $\nu$ ($cm^{-1}$) | $\Gamma_{FWHM}$ ($cm^{-1}$) |
| 0.1 | 1695.8 | 16.1 | 1712.4 | 18.8 | – | – | 1728.7 | 14.6 |
| 0.2 | 1696.5 | 15.9 | 1713.7 | 20.7 | – | – | 1729.7 | 14.0 |
| 0.3 | 1695.2 | 14.9 | 1713.1 | 23.0 | – | – | 1729.1 | 13.8 |
| 0.4 | 1695.4 | 16.0 | 1713.1 | 21.2 | – | – | 1729.0 | 13.6 |
| 0.5 | 1695.3 | 15.0 | 1713.1 | 21.8 | – | – | 1728.9 | 13.2 |
| 0.6 | 1691.5 | 16.3 | – | – | 1720.5 | 18.1 | 1731.3 | 13.1 |
| 0.7 | 1692.4 | 18.4 | – | – | 1720.6 | 18.1 | 1731.6 | 12.7 |
| 0.8 | 1691.1 | 16.7 | – | – | 1720.7 | 16.6 | 1731.6 | 12.3 |
| 0.9 | 1690.3 | 15.8 | – | – | 1721.1 | 14.9 | 1731.8 | 12.1 |
| 1.0 | 1689.3 | 14.9 | – | – | 1721.6 | 12.3 | 1731.8 | 12.0 |

Journal of RAMAN SPECTROSCOPY

**Table 3.** Wavenumber positions and line widths of the three Raman peaks obtained by analyzing the observed isotropic Raman line profile in the $\nu$(C═O) region at different concentrations in mole fraction *C* of propanal in the (Pr + M) binary mixture

| Mole fraction (*C*) (propanal) | Peak 1 | | Peak 2 (C═O)$_{HB}$ | | Peak 3 (C═O)$_{SA}$ | | Peak 4 (C═O)$_{ISO}$ | |
|---|---|---|---|---|---|---|---|---|
| | $\nu$ (cm$^{-1}$) | $\Gamma_{FWHM}$ (cm$^{-1}$) | $\nu$ (cm$^{-1}$) | $\Gamma_{FWHM}$ (cm$^{-1}$) | $\nu$ (cm$^{-1}$) | $\Gamma_{FWHM}$ (cm$^{-1}$) | $\nu$ (cm$^{-1}$) | $\Gamma_{FWHM}$ (cm$^{-1}$) |
| 0.2 | 1695.9 | 16.1 | 1722.8 | 21.2 | – | – | 1734.4 | 14.1 |
| 0.3 | 1695.1 | 16.4 | 1723.3 | 24.2 | – | – | 1734.4 | 14.4 |
| 0.4 | 1693.3 | 14.2 | 1718.4 | 17.4 | 1728.5 | 10.4 | 1736.0 | 11.3 |
| 0.5 | 1692.7 | 15.8 | 1718.0 | 17.7 | 1728.4 | 12.3 | 1736.1 | 12.7 |
| 0.6 | 1692.9 | 16.6 | 1717.1 | 17.2 | 1726.9 | 15.0 | 1734.7 | 13.9 |
| 0.7 | 1692.0 | 16.9 | 1719.3 | 17.5 | 1726.8 | 17.7 | 1734.1 | 12.0 |
| 0.8 | 1692.0 | 13.7 | – | – | 1725.0 | 25.4 | 1734.8 | 8.6 |
| 0.9 | 1690.3 | 16.7 | – | – | 1722.0 | 16.4 | 1732.6 | 14.9 |
| 1.0 | 1689.3 | 14.9 | | – | 1721.6 | 12.3 | 1731.8 | 12.0 |

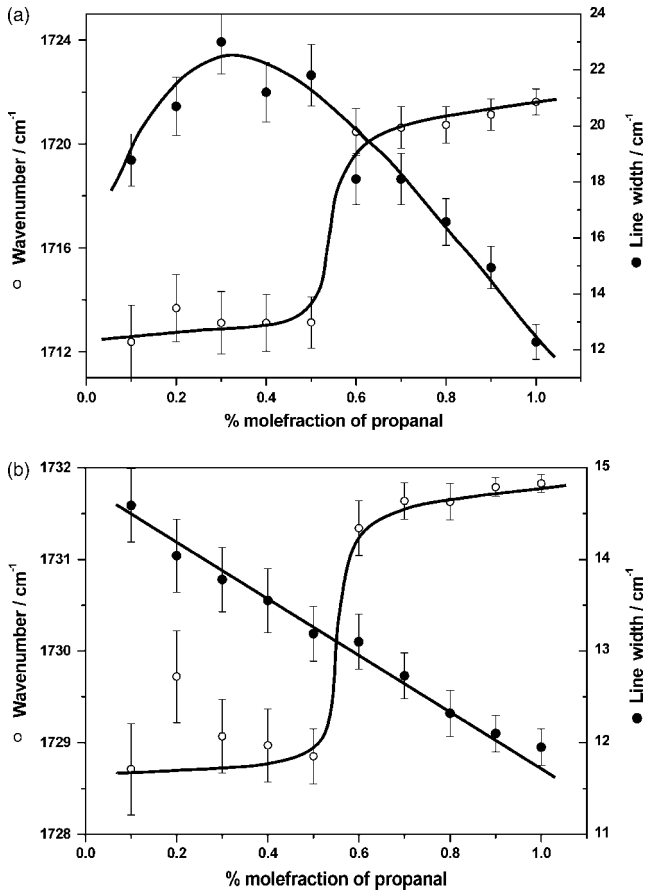


**Figure 7.** Variation of peak positions and line widths of the Raman Peak 2 and Raman Peak 3 as a function of concentration *C* (same as in Fig. 1) in the [Pr + W] binary mixture: (a) Peak 2 and (b) Peak 3.

The concentration-dependent Raman study of the (Pr + M) binary mixture shows a rather regular trend of wavenumber shift in contrast to the concentration dependence of spectral features in the Raman study of the (Pr + W) binary mixture. One of the reasons for a relatively smooth spectral variation is good solubility of Pr in M. The change in spectral features with concentration shows that the intensity of the Raman band due to self-associated dimer of neat Pr at ~1721 cm$^{-1}$ diminished considerably on higher dilution (Fig. 2) and a new band starts appearing on the low wavenumber side at ~1719 cm$^{-1}$, the intensity of which goes on increasing upon dilution. It clearly shows that the new band is due to the formation of the (Pr + M) complex, such as $PrM_3$, as shown in Fig. 4(g) with calculated wavenumber of the $\nu$(C═O) stretching vibration at 1753 cm$^{-1}$, which is also lower than the calculated wavenumber of the $\nu$(C═O) stretching vibration of the self-associated complex (1774 cm$^{-1}$). As a consequence, the proportion of self-associated complex in the mixture goes on decreasing with dilution and ultimately tends to disappear at high dilution, one of the reasons for disappearance being the formation of more number of hydrogen-bonded complexes and the other being the steric hindrance produced by the methyl group of M in forming the self-associated complexes. Thus the Raman spectra of the binary mixture at high dilution contain only contributions from $\nu$(C═O) stretching vibrations of (Pr + M) complexes and from the isolated Pr molecules.

## Conclusions

Hydrogen-bonding interaction of Pr with the hydrogen-donor solvents W and M was studied in the binary mixtures (Pr + W) and (Pr + M). The C═O stretching region of neat Pr also exhibits a doublet feature in the Raman spectra with two peaks at ~1721 and ~1732 cm$^{-1}$, which are attributed to the C═O stretching vibration of the self-associated and isolated Pr species, respectively. The peak corresponding to the self-association was confirmed by the Raman study of Pr in the C═O stretching region, with a noninteracting solvent, *n*-heptane. A significant decrease in the intensity of this band (~1721 cm$^{-1}$) at high dilution with *n*-heptane clearly indicates that this peak corresponds to the self-associated species. The wavenumber shift and line width variation with concentration of Pr in the different mixtures clearly show that the Raman bands corresponding to C═O stretching vibration of the isolated as well as self-associated species show a red shift upon dilution with W as well as with M. DFT calculations also show that in the presence of hydrogen-donor solvents W or M, the Pr molecule makes hydrogen bonds; the formation of these hydrogen bonds weakens the C═O bond and consequently shows a red shift in the Raman spectra. Thus, in conclusion, a combined study of both Raman and DFT calculations gives a clear evidence of isolated, self-associated and hydrogen-bonded species of Pr existing in the binary mixtures (Pr + W) and (Pr + M) and of a certain equilibrium existing at each concentration.



  

**Acknowledgements**

BPA, SKS and RKS are thankful to the Alexander von Humboldt Foundation for support in different forms. DKS is thankful to the University Grant Commission, India, for the Research Fellowship in Science for Meritorious Students (UGC-RFSMS).

## References

[1] G. A. Jeffrey, W. Saenger, *Hydrogen Bonding in Biological Structures*, Springer: Berlin, **1991**.
[2] G. C. Pimentel, A. L. McClellan, *The Hydrogen Bond*, Freeman: San Francisco, **1960**.
[3] C. L. Perrin, J. B. Nielson, *Annu. Rev. Phys. Chem.* **1997**, *48*, 511.
[4] A. J. Kirby, *Acc. Chem. Res.* **1997**, *30*, 290.
[5] S. Schlund, M. Mladenovic, E. M. Basílio Janke, B. Engels, K. Weisz, *J. Am. Chem. Soc.* **2005**, *127*, 16151.
[6] H. S. Andrei, N. Solca, O. Dopfer, *Chem. Phys. Chem.* **2006**, *7*, 107.
[7] B. P. Asthana, W. Kiefer, in *Vibrational Spectra and Structure*, vol. 20 (Ed: J. R. Durig), Elsevier: Amsterdam, **1993**, p 69.
[8] U. W. Suter, *J. Am. Chem. Soc.* **1979**, *101*, 6481.
[9] M. R. Peterson, G. R. Demare, G. Csiz-Madia, O. P. Straust, *J. Mol. Struct.* **1983**, *92*, 239.
[10] N. G. Rondan, M. N. Paddon-Ron, P. Caramella, K. N. Houk, *J. Am. Chem. Soc.* **1981**, *103*, 2436.
[11] N. L. Allinger, M. J. Hickey, *J. Mol. Struct.* **1973**, *17*, 233.
[12] G. Sbrana, V. Schettino, *J. Mol. Spectrosc.* **1970**, *33*, 100.
[13] P. Van Nuffel, L. Van den Enden, C. Van Alsenoy, H. J. Geise, *J. Mol. Struct.* **1984**, *116*, 99.
[14] K. B. Wiberg, E. Martin, *J. Am. Chem. Soc.* **1985**, *107*, 5035.
[15] G. Frenking, K. F. Kohler, M. T. Reetz, *Tetrahedron* **1991**, *47*, 8991.
[16] A. Vivier-Bunge, V. H. Uc, F. J. Mele'ndez, Y. G. Smeyers, *Folia Chim. Theoret. Lat.* **1995**, *23*, 186.
[17] G. P. Kolandaivel, N. Kuze, N. Ponmalai, T. Sakaizumi, O. Ohashi, K. Iijima, *J. Phys. Chem. A* **1997**, *101*, 2873.
[18] A. Zanoun, V. Durier, A. Belaidi, G. Vergoten, *J. Mol. Struct.* **1999**, *476*, 261.
[19] A. V. Kudich, V. A. Bataev, A. V. Abramenkov, V. I. Pupyshev, I. A. Godunov, *J. Mol. Struct. (Theochem)* **2003**, *631*, 39.
[20] M. Hwa Kim, L. Shen, A. G. Suits, *Phys. Chem. Phys. Chem.* **2006**, *8*, 2933.
[21] M. Villa, M. L. Senent, R. Dominguez-Gomez, *Chem. Phys. Lett.* **2007**, *436*, 15.
[22] S. Choi, T. Y. Kang, K. W. Choi, S. Han, D. S. Ahn, S. J. Baek, K. S. Kim, *J. Phys. Chem. A* **2008**, *112*, 5060.
[23] A. Morresi, L. Mariani, M. R. Distefano, M. G. Giorgini, *J. Raman Specrosc.* **1995**, *26*, 179.
[24] B. P. Asthana, H. Takahashi, W. Kiefer, *Chem. Phys. Lett.* **1983**, *94*, 41.
[25] B. P. Asthana, W. Kiefer, E. W. Knapp, *J. Chem. Phys.* **1984**, *81*, 3774.
[26] V. Deckert, B. P. Asthana, W. Kiefer, H.-G. Purrucker, A. Laubereau, *J. Raman Spectrosc.* **2000**, *31*, 805.
[27] B. P. Asthana, V. Deckert, M. K. Shukla, W. Kiefer, *Chem. Phys. Lett.* **2000**, *326*, 123.
[28] A. Morresi, P. Sassi, M. Paolantoni, S. Santini, R. S. Cataliotti, *Chem. Phys.* **2000**, *254*, 337.
[29] M. J. Frisch, G. W. Trucks, H. B. Schlegel, G. E. Scuseria, M. A. Robb, J. R. Cheeseman, V. G. Zakrzewski, J. A. Montgomery Jr, R. E. Stratmann, J. C. Burant, S. Dapprich, J. M. Millam, A. D. Daniels, K. N. Kudin, M. C. Strain, O. Farkas, J. Tomasi, V. Barone, M. Cossi, R. Cammi, B. Mennucci, C. Pomelli, C. Adamo, S. Clifford, J. Ochterski, G. A. Petersson, P. Y. Ayala, Q. Cui, K. Morokuma, D. K. Malick, A. D. Rabuck, K. Raghavachari, J. B. Foresman, J. Cioslowski, J. V. Ortiz, A. G. Baboul, B. B. Stefanov, G. Liu, A. Liashenko, P. Piskorz, I. Komaromi, R. Gomperts, R. L. Martin, D. J. Fox, T. Keith, M. A. Al-Laham, C. Y. Peng, A. Nanayakkara, M. Challacombe, P. M. W. Gill, B. Johnson, W. Chen, M. W. Wong, J. L. Andres, C. Gonzalez, M. Head-Gordon, E. S. Replogle, J. A. Pople, *Gaussian 03*, Gaussian, Inc., Pittsburgh, PA, **2003**.
[30] A. D. Becke, *J. Chem. Phys.* **1992**, *97*, and **1993**, *98*, 5648.
[31] C. Lee, W. R. Yang, G. Parr, *Phys. Rev. B* **1988**, *37*, 785.
[32] D. K. Singh, S. K. Srivastva, A. K. Ojha, B. P. Asthana, *Spectrochim. Acta A* **2008**, *71*, 823.
[33] D. K. Singh, S. K. Srivastva, A. K. Ojha, B. P. Asthana, *J. Mol. Struct.* **2008**, *892*, 384.
[34] B. Mennucci, J. Tomasi, *J. Chem. Phys.* **1997**, *106*, 5151.
[35] D. W. Oxtoby, *Adv. Chem. Phys.* **1979**, *40*, 1.
[36] P. A. Egelstaff, *An Introduction to Liquid State*, Academic Press: New York, **1967**.